BioNanoScience (2021) 11:526–538
https://doi.org/10.1007/s12668-021-00846-1

Green Phytosynthesis of Silver Nanoparticles Using *Echinochloa stagnina* Extract with Reference to Their Antibacterial, Cytotoxic, and Larvicidal Activities

Amr M. Shehabeldine[1] · Mostafa A. Elbahnasawy[1] · Ahmed I. Hasaballah[2]

Accepted: 15 February 2021 / Published online: 22 February 2021

Abstract
Herein, we report a novel green phytosynthesis for silver nanoparticles (AgNPs) using *Echinochloa stagnina* (Retz.) P. Beauv. (Burgu) extract and assess their potential activities. The phytosynthesized AgNPs were characterized using UV-visible spectroscopy, X-ray diffraction (XRD), transmission electron microscopy (TEM), dynamic light scattering (DLS), and Fourier transform infrared (FTIR) spectroscopy. The surface plasmon resonance was peaked at 405 nm indicating the formation of AgNPs. Morphologically, AgNPs were spherical in shape with a diameter of 30 nm and monodispersed. Structurally, XRD data indicated that AgNPs were highly nanocrystalline in nature. FTIR spectral analysis demonstrated the presence of phytochemicals which could be responsible for the reduction of Ag ions and capping of AgNPs. The phytosynthesized AgNPs showed antibacterial activity with MIC of 12.5 and 6.25 μg/mL against multidrug-resistant (MDR) *Klebsiella oxytoca* (ATCC 51983) and *Pseudomonas aeruginosa* (ATCC MP-23), respectively. The time-kill kinetics profile of AgNPs against MDR *Klebsiella oxytoca* (ATCC 51983) and *Pseudomonas aeruginosa* (ATCC MP-23) revealed a time- and dose-dependent reduction manner. The inhibition concentrations of AgNPs that inhibits 50% (IC_{50}) of Vero and HepG2 cells were 89.01 and 35.1 μg/mL, respectively. The LC_{50} and LC_{90} concentrations were (87.669 and 538.017 mg/mL) for *Anopheles pharoensis* and (51.338 and 311.227 mg/mL) for *Culex pipiens*, respectively. Collectively, our data suggest that plant-mediated synthesis of AgNPs is more feasible to synthesis AgNPs with improved properties.

Keywords Green synthesis · AgNPs · Burgu grass · Antibacterial activity · MDR · HepG2 · Larvicidal activity

1 Introduction

Nanotechnology is a highly revolutionized field for generating novel and promising therapeutic nanomaterials in diverse medical applications, e.g., nanomedical devices, household products, clothing, room sprays or, even food products [1–3]. In the last few years, silver nanoparticles (AgNPs) have attracted more attention due to their extraordinary biological activities against microorganisms. AgNPs have shown tremendous applications in wound healings, drug delivery, cosmetics, bio-labeling, food preservation, water purifications, paints, textiles, catalysis, and electronics [4]. Silver particles would exhibit novel and promising chemical and biological properties in their nanoscale sizes due to their higher surface area and energy compared to raw silver particles [5]. Several physical, chemical, and biological approaches have been demonstrated for a better synthesis of AgNPs with high yield, solubility, and stability. At present, plant-mediated synthesis of AgNPs is an emerging, developing, and attractive research area due to cost-effectiveness, eco-friendly, biodegradability, and low toxicity and various secondary metabolites offered by plants [6–9]. Plants, particularly medicinal ones, are reservoirs for many bioactive compounds. Unfortunately, several limitations have been associated with herbal drugs usage including size, poor absorption, and reduced compatibility. In recent years, integration of medicinal plants with nanotechnology applications promoted the therapeutic efficiency of medicinal plants/herbal drugs in various human diseases [10]. Production of AgNPs by plant extracts could generate AgNPs with improved properties coming from the synergetic effect of combination of both AgNPs and plant bioactive

✉ Mostafa A. Elbahnasawy
Mostafa.elbahnasawy@azhar.edu.eg

[1] Botany and Microbiology Department, Faculty of Science, Al-Azhar University, Nasr City, Cairo 11884, Egypt

[2] Zoology and Entomology Department, Faculty of Science, Al-Azhar University, Nasr City, Cairo 11884, Egypt

ingredients. Therefore, plant-mediated AgNPs have shown high biological activities than others produced by traditional methods [11].

Plant extracts contain various biomolecules which functioning as not only reducing agents for reducing Ag to AgNPs, but also capping/stabilizing agents for preventing the aggregation of the formed AgNPs, thus providing their stability. These reducing biomolecules include proteins, vitamins, polysaccharides, fats, enzymes, polyphenols, flavonoids, alkaloids, and terpenoids. More detail, previous plant extract metabolites contain functional groups like hydroxyl (OH), carbonyl (CO), amine (NH_2), and methoxide (CH_3O) which react with silver precursor [12]. *Echinochloa stagnina* (Retz.) P. Beauv. (Burgu) is a semi-aquatic fast-growing grass widespread in tropical regions. It is an important and economic crop used for desalinization of saline lands [13]. Because of its high sugar content, Burgu is considered an excellent fodder grass and in beverages production. It contains proteins, fiber, fat, nitrogen-free extracts, sugars, and elements (Ca, Mg, and P) [14].

Multidrug-resistant (MDR) bacteria are serious threats to global public health, due to their wide-spreading behind nosocomial to community-associated bacteria causing community-acquired infections [15, 16]. With the current few treatment options exist for people infected with MDR bacteria, researchers are looking for a new effective antimicrobial agent against MDR bacteria with less toxicity towards humans. The actual mechanism of antibacterial action of AgNPs is not yet completely known; previous reports stated that it could be due to the electrostatic attraction between bacterial cells (negative charge) and nanoparticles (positive charge) [17]. Among vectors of diseases of much interest are mosquitoes, which cause millions of deaths every year globally. *Culex pipiens* is a very important mosquito species that inhabits many regions worldwide including Egypt; it transmits several diseases such as lymphatic filariasis which alone cause about 120 million infection and 44 million chronic manifestation [18]. *Anopheles pharoensis* **is** consider**ed a** main vector of malaria disease that cause about 1.5–2.7 million death annually [19] that led to both economic and developmental loss for both national and international levels. Chemical insecticides are harmful primarily for the environment and for non-targeted organism/microorganisms, and their increased use made these insecticides less effective mosquito control agents and consequently allow mosquito-borne diseases outbreak [20–23]. Therefore, there is a critical need to develop an effective and eco-friendly larvicide/insecticide agent to control such mosquito-borne disease outbreaks. Botanical extracts that possess larvicidal properties represent novel promising pesticides that able to control vectors/pests with less toxicity to the non-target organisms and at the same time less pollutant to the environmental [24]. Larvicides from botanical origin contain usually many chemical compounds, if compared to conventional insecticides, that affect different biological aspects and also reveal reduced developed resistance in their targets [25]. Alternative to these botanical larvicides is the green synthesis of AgNPs using plant extracts. There are increased demands of green biosynthesized nanoparticles from natural origin such as plant or plant-derived metabolites as larvicide or insecticide agents to help reducing mosquito populations [26]. In sum, these characteristics encourage researchers to synthesize and develop novel AgNPs with valuable properties.

This study aims to develop a clean, cheap, and effective approach for green phytosynthesis of AgNPs using *Echinochloa stagnina* (Retz.) P. Beauv. (Burgu) extract and investigate their potentially therapeutic properties. Phytosynthesized AgNPs were evaluated for antibacterial activity against MDR gram-negative bacteria, cytotoxicity effect against Vero and HepG2 cells, and the potential larvicidal activity against different tested mosquito species.

2 Materials and Methods

2.1 Bacterial Strains and Reagents

Extended-spectrum beta-lactamase (ESBL) *Klebsiella oxytoca* ATCC 51983 and drug-resistant *Pseudomonas aeruginosa* Panel ATCC MP-23 were purchased from American Type Culture Collection (ATCC). Silver nitrate, ciprofloxacin, and sodium hydroxide (NaOH) were obtained from Sigma-Aldrich (St. Louis, MO, USA) and Merck (Darmstadt, Germany).

2.2 Preparation of Plant Extract and Synthesis of AgNPs

The shoots of Burgu grass (*Echinochloa stagnina* (Retz.) P. Beauv.) were collected from Kafr Al-zayat, Gharbiah governorate, Egypt (longitude 30° 48′ 07″ E and latitude 30° 51′ 05″ N), washed with sterile double distilled water thoroughly for 2–3 times until no impurities remained, dried out at room temperature, cut into small pieces, and ground using grinder. Then, Burgu powder (5 g) was suspended in sterile deionized distilled water (100 mL) and heated up to 70°C for 10 min. The cooled solution of Burgu extract was filtered with Whatman No. 1 filter paper and centrifuged (3500 rpm, 20 min). Soon after, the collected supernatant was used as a reducing and stabilizing agent for production of AgNPs from $AgNO_3$ precursor solution. The fresh Burgu extract (pH 7) was mixed with $AgNO_3$ solution (1 mM) at a ratio of 1:9 (v/v), respectively, and kept in dark at room temperature for overnight or until the solution color turn to brown. Burgu extract solution was included without addition of $AgNO_3$ as a control, showing no color changes.

2.3 Characterization of Synthesized AgNPs

Formation of AgNPs was firstly characterized by UV-visible (UV-vis) Spectroscopy (Shimadzu UV-1700, Japan) at scanning range from 300 to 700 nm. The morphology of AgNPs was determined by transmission electron microscopy (TEM). Briefly, a drop (3 μL) of AgNPs solution was placed on a carbon-coated copper grid, dried under infrared lamp, and examined by a JEOL 1010 TEM (Japan) at a voltage of 200 kV. The average particle size and size distribution of AgNPs were determined by dynamic light scattering (DLS) (The Nicomp ZLS Z 3000, USA). For DLS, the AgNP solution was diluted tenfold by PBS (pH 7.4) and the measurements were taken in the range between 0.1 and 10,000 nm. The X-ray diffraction (XRD) was used to determine the crystallite nature of AgNPs. XRD measurements of the dried powder AgNPs were done by X-ray diffraction system Shimadzu LabX XRD-6000 with a Cu-Kα X-ray source (λ= 1.5418Å). The crystallite domain size (D) of AgNPs was calculated using the Debye–Scherrer's formula: D= Kλ/β Cosθ, where K is the shape factor (0.9), λ is the wavelength of the used X-ray source for diffraction, β is the full width half maximum (FWHM) of diffraction peak in Radians, and θ is the diffraction angle at that intensity. Uncapped and free residues that did not attached to nanoparticles were removed by centrifugation (3 times, 15000 rpm, 20 min). Finally, Fourier transform infrared (FTIR) spectroscopy (Perkin-Elmer FTIR-1600, USA) was used for detection of functional groups that could be responsible for reduction of silver ions to AgNPs. The air-dried AgNPs (300 μL) was mixed with potassium bromide (10 mg) and then oven dried. The FTIR spectra were taken range of 500–4000 cm^{-1} at a resolution of 4 cm^{-1}.

2.4 Antibacterial Activity of AgNPs

Antibacterial activity of green-synthesized AgNPs was determined in vitro using the disk diffusion method [27]. Human pathogenic multidrug-resistant bacteria *Klebsiella oxytoca* ATCC 51983 and *Pseudomonas aeruginosa* ATCC MP-23 were used for this analysis. Strains were grown in Mueller-Hinton broth medium at 37°C for 18 h with shaking. As a reference, the 0.5 McFarland standard ($BaSO_4$ turbidity) was included to count *K. oxytoca* and *P. aeruginosa* cell numbers. A volume of 100 μL of overnight-grown culture of each strain (McFarland turbidity of 0.5) was spread onto Mueller-Hinton agar (MHA) plates and sterilized 6-mm filter paper disks loaded with 50 μL of AgNPs (25 or 50 μg/mL) were aseptically placed on the middle of plates, and plates were incubated at 37°C for 24 h. Ciprofloxacin (5 μg/mL) and silver nitrate solution were utilized as positive and negative controls, respectively. Following the incubation, the radius of the inhibition zone was measured by using a vernier caliper and scored for antibacterial activity.

Minimal inhibitory concentrations (MIC) of AgNPs against *K. oxytoca* ATCC 51983 and *P. aeruginosa* ATCC MP-23 were assessed by microbroth dilution method using resazurin dye [28]. Micro-dilution of overnight grown culture strains (McFarland turbidity of 0.5) were cultured in 96-well plates using Muller-Hinton broth medium. Different concentrations of AgNPs (50, 25, 12.5, 6.25, 3.12, and 1.56 μg/mL) were added and plates were incubated at 37°C for overnight. Then, 30-μL resazurin solution (0.1 mg/mL) was added to each well and incubated at 37°C for at least 2 h. Any change in culture color from blue dye to pink within viable cells was assessed visually [29]. The lowest concentration of AgNPs in which the change in dye's color occurred was taken as the MIC value. Minimum bactericidal concentration (MBC) of AgNPs was also determined by sub-culturing *K. oxytoca* and *P. aeruginosa* from MIC plates, particularly wells followed the MIC values, into MHA plates at 37°C for 24 h. Then, MBC was detected as the lowest concentration of AgNPs that prevent the growth of *K. oxytoca* and *P. aeruginosa*. The action of AgNPs as antibacterial activity on tested bacteria can be described by the ratio of MBC/MIC. When the ratio equals to 1 or 2, it means bactericidal effect, and when the ratio is ≥4, it means bacteriostatic effects [30].

2.5 Time-Kill Kinetics

Time-kill kinetics assay of AgNPs was carried out as described by Keepers et al. [30]. Briefly, overnight grown colonies of each strain (*K. oxytoca* and *P. aeruginosa*) were resuspended and incubated (37°C, 180 rpm) for 2 h. An inoculum size of 1×10^6 CFU/mL of each strain (*K. oxytoca* and *P. aeruginosa*) was inoculated into sterilized Luria-Bertani (LB) broth media, followed by addition of successive concentrations of AgNPs MIC (0.5×MIC, 1×MIC, 2×MIC, 4×MIC, and 8×MIC), and then incubated (37°C, 180 rpm). A growth control with no AgNPs was also included. Aliquots of 1 mL of cultures were taken at time intervals of 0, 15, 30, 60, and 120 h and were spread onto LB agar plates and incubated at 37°C for 24 h. The viable cells were counted as CFU/mL.

2.6 Cell Viability and Cytotoxic Activity of AgNPs

The in vitro potential cytotoxic activity of AgNPs against normal Vero cell line and human hepatocellular carcinoma cell line HepG2 (ATCC HB-8065), which is recognized as a standard model for cytotoxicity evaluating studies. HepG2 and Vero cells were cultured in Dulbecco's Modified Eagle Medium (DMEM) supplemented with l-glutamine (2.9 mg/mL), penicillin-streptomycin, and 10% fetal calf serum. At 90% confluence, the cells were harvested using 0.25% trypsin EDTA at 37°C. Different concentrations of AgNPs were evaluated against

normal cell line (Vero cell lines) and tumor cells (HepG2). AgNPs were diluted in a series of twofold concentrations (5, 10, 20, 40, 80, 160, 320, and 640 μg/mL), followed by incubation at 37 °C and 5% CO2 for 48 h. Cell damage induced by sliver nanoparticles was morphologically observed under a Carl Zeiss inverted microscope (GmbH, Germany). The cytotoxicity activities were investigated using a 3-(4,5-dimethylthiazol-2-yl)-2,5-diphenyltetrazolium bromide (MTT) assay [31]. One hour after incubation with MTT, it is reduced to purple formazan crystals by the living cells and quantitated at 570 nm, using an ELISA. Concentrations of AgNP showing 50% reduction in cell viability (IC_{50} [half maximal inhibitory concentration] values) were then calculated. Each experiment was performed in triplicate and the relative cellular viability percentage was calculated using the following formula:

$$\text{Cell viability\%} = \left(\frac{\text{OD treated cells}-\text{OD balnk}}{\text{OD untreated cells}-\text{OD balnk}}\right) \text{x } 100$$

2.7 Mosquito Culture

Anopheles pharoensis and *Culex pipiens* eggs were provided by the Medical Entomology Research Centre. Egg masses were separately reared in white plastic bowl (30 cm in diameter) containing 500-mL tap water under maintained laboratory conditions of 27±2°C, 70±5% relative humidity, and 14–10 h light and dark regimen. The hatched larvae were daily provided with fish food as a diet.

2.8 Mosquito Larvicidal Bioassay

The larvicidal bioassay of biosynthesized AgNPs was estimated for *An. pharoensis* and *C. pipiens*. Ten early third instar larvae of both tested mosquitoes were placed in disposal paper cups (its capacity 200 mL) containing 100-mL tap water. AgNPs were added at serial concentrations of 50, 100, 200, 300, 400, 500, and 600 mg/L with three replicates, in addition to the control were tested at the laboratory conditions. The mortality of treated larvae with AgNPs was recorded at 24 h post-treatment.

2.9 Statistical Analysis

Descriptive statistics including mean, standard deviation (SD), CIs, and Chi-square were calculated using SPSS ver. 25. Probit analysis was used for LC_{50} and LC_{90} determination. Data was presented as mean ± SD. *P* value was considered significant at < 0.05.

3 Results and Discussion

In recent years, plant-mediated synthesis of AgNPs has been attracted much of interest as the best biological-mediated system for fabrication of nanoparticles [6]. This method is more feasible due to its high eco-friendly aspects, energy saver, nontoxicity, scalable up, lower costs, time saver, and simple to purify compared to other conventional approaches, such as physical, chemical and microorganisms-mediated methods [7–9]. The later methods require high aseptic conditions, long time, and purification. Physico-chemical characterization of generated AgNPs is an essential initial step to recognize their size, shape, homogeneity, surface area, and surface chemistry. This would provide great information on nanoscale process, potential properties of the nanoparticles produced, and insight into control of AgNPs properties, via improving their rate of synthesis and quality, for desired and wider applications.

3.1 Characterization of AgNPs

It is well-established that formation of AgNPs could be visually detected by color change of reaction to yellowish brown color. AgNPs per se possess unique optical properties which strongly interact with some particular wavelengths of light, resulting in a characteristic surface plasmon resonance (SPR) peak between 400 and 450 nm. In the present study, the fresh Burgu extract was turned to brownish color after 14 h of incubation with the aqueous solution of silver nitrate ($AgNO_3$), indicating the reduction of silver ions to AgNPs. It is known that when the surface plasmon vibrations in AgNPs are excited, the AgNPs exhibit some yellowish brown color in aqueous solutions. The control silver nitrate solution (without Burgu extract) showed no change of color. The characteristic absorption peak at 405 nm in UV-visible spectrum (scanning range 300–700 nm) confirmed the formation of AgNPs (Fig. 1a). Similarly, formation of AgNPs has been monitored by giving SPR peaks at 400 nm [32], 410 nm [33], 418 nm [34], 420 nm [35], 430 nm [36], and 450 nm [37].

The morphology of phytosynthesized AgNPs by Burgu extract was recovered from the TEM as displayed in Fig. 1b. The TEM micrograph images exhibited that AgNPs were monodispersed and spherical in shape with a particle size ranged between 18 and 39 nm and an average size of 30 nm. The monodispersing of AgNPs implies that AgNPs are bounded by an organic layer, suggesting that some capping/adhering phytochemical agents from Burgu extract are involved in the biosynthesis process of AgNPs [38]. The non-agglomeration of nanoparticles plays an essential role in achieving high efficiency of application purposes of nanoparticles. TEM micrographs showed monodispersed spherical AgNPs (28.7±4.5 nm) without any apparent changes after 30 days which indicates the stability of biosynthesized

colloidal AgNPs (Fig. 1c). The size of phytosynthesized AgNPs and their distributions were further observed by DLS with respect to the volume and number of AgNPs (Fig. 1d). The DLS analysis revealed monodispersed AgNPs with a variance or polydispersity index of 0.307 and AgNP size distributions from 18 to 30 nm (mean diameter 21.8±2.9 nm, 20.1 ±2.4 nm, and 19.5±2.7 nm for intensity, volume, and number, respectively). The acquired particle size distribution value was in good accordance with particle size received from TEM analysis.

The nanocrystalline nature of phytosynthesized AgNPs was identified by XRD analysis. The XRD spectral data of AgNPs exhibited four intense Bragg's reflection peaks in the whole spectrum of 2θ values ranging from 10 to 80 (Fig. 1e). The XRD reflection peaks at 2θ degree were 31.7, 45.6, 56.6, and 75.3 correspond to the (111), (200), (220), and (311) crystalline planes, indicating the face-centered cubic crystalline structure of metallic silver particles (JCPDS, File No. 04–0783). The XRD pattern strongly revealed that phytosynthesized AgNPs were nanocrystalline in nature. The present XRD peaks were reported in many works confirming the nanocrystalline nature of AgNPs [36–40]. Similar data were reported by Dakshayani et al. [36] which synthesized AgNPs by using *Selaginella bryopteris* plant extract. Pirtarighat et al. [37] used plant extract of *Ocimum basilicum* as a reducing and capping agent for biosynthesis of AgNPs. Prasannaraj et al. [39] used plant extracts of *Plumbago zeylanica*, *Semecarpus anacardium*, and *Terminalia arjuna* to fabricate AgNPs. Elmusa et al. [40] used plant extract obtained from *Abelmoschus esculentus* to produce AgNPs. Following the Scherer's equation, the crystal size of AgNPs was ranged from 23.4 to 59.5 nm with an average of 38 nm. The average crystallite size value was in good accordance with particle size received from DLS and TEM analyses.

The FTIR measurements were conducted to reveal the functional phytochemical groups and identify the potential phyto-biomolecules that probably participated in the bioreduction of silver ions and stabilization of AgNPs. The FTIR spectrum of phytosynthesized AgNPs by Burgu extract is shown in Fig. 1f. The FTIR spectral analysis revealed 11 distinct absorption bands at 3425, 2958, 2283, 2133, 1640, 1400, 1246, 1095, 926, 613, and 528 cm^{-1}. The broad peak observed at 3425 cm^{-1} could be attributed to the stretching vibrations of free OH group in polyphenols and alcohols, while the band at 1400 cm^{-1} corresponds to bending of OH side group present in amino acid residues of the protein molecules [36, 37]. During the reduction of Ag precursors, polyphenols act as strong antioxidants and hydrogen donors. As a redox reaction, hydroxyl (OH) groups in reduced polyphenols are then turn to carbonyl (CO) groups which strongly bind and stabilize AgNPs [41]. The vibrational peak at 2958.3 cm^{-1} is corresponding to characteristic to CH vibrational stretching in aliphatic methyl and methylene [36]. The strong bands at 2283 and 2133 cm^{-1} are due to N=C=O (isocyanate) and N=N=N (azide) stretching, respectively. The characteristic bands recorded at 1640 cm^{-1} are due to the carbonyl (C=O) stretching vibration of amide I [39, 42]. It has been demonstrated that proteins attach to metal nanoparticles through their free amide groups, due to the intrinsic strong affinity of their carbonyl groups to bind metals via electrostatic interaction and thus initiating the reduction process. Therefore, the presence of C=O in the FTIR spectrum indicates that AgNPs are encapsulated by proteins and peptides originated from Burgu extract, which prevent agglomeration and thereby stabilize the AgNPs in medium. The absorption band at 1245 cm^{-1} is assigned for C-N stretching of amide III, while the band at 1095 cm^{-1} is due to the stretching vibrations of C-C group found in sugars and fats in the Burgu extract. The band localized at 925 cm^{-1} can be attributed to either sulfur or phosphorus function groups, which possibly attach to AgNPs as a capping and stabilizing agent. The peaks at 626 and 528 cm^{-1} indicate the bending region of the aliphatic chain. Overall, FTIR spectroscopic data confirmed that the Burgu extract has the ability to perform dual functions of bioreduction and stabilization of silver nanoparticles, thus preventing the AgNPs from adhering and agglomerating. To the best of our knowledge, this is the first study reporting using of Burgu extract as a reducing and stabilizing agent for synthesis of AgNPs.

3.2 Antibacterial Activity of AgNPs

3.2.1 Determination of Antimicrobial Activity of Synthesized AgNPs

The preliminary detection of the biosynthesized AgNPs against human pathogenic multidrug-resistant gram-negative bacteria, *K. oxytoca* (ATCC 51983) and *P. aeruginosa* (ATCC MP-23), was done using disk diffusion method and microbroth dilution assay. Both of *P. aeruginosa* and *K. oxytoca* were selected due to their outstanding resistance to various antibiotics. The diameters of inhibition zones are summarized in Table 1 and illustrated in Fig. 2. Results suggested that the highest concentration of AgNPs had a greater inhibition activity against both tested strains *K. oxytoca* and *P. aeruginosa* with 15- and 19-mm inhibition zones, respectively, at 50 μg/mL, which consider the lowest concentration if compared with previous AgNP studies [43, 44].

The MIC is the minimum concentration of AgNPs required for inhibition of the visible growth of microbes [45]. Our results showed that MIC of AgNPs were 6.25 and 12.5 μg/mL against *K. oxytoca* and *P. aeruginosa*, respectively (Table 1). The higher diameter of inhibition zone observed with lower MIC values proved good antibacterial activity using resazurin-mediated microtiter plate assay. The advantages of this assay in detection of

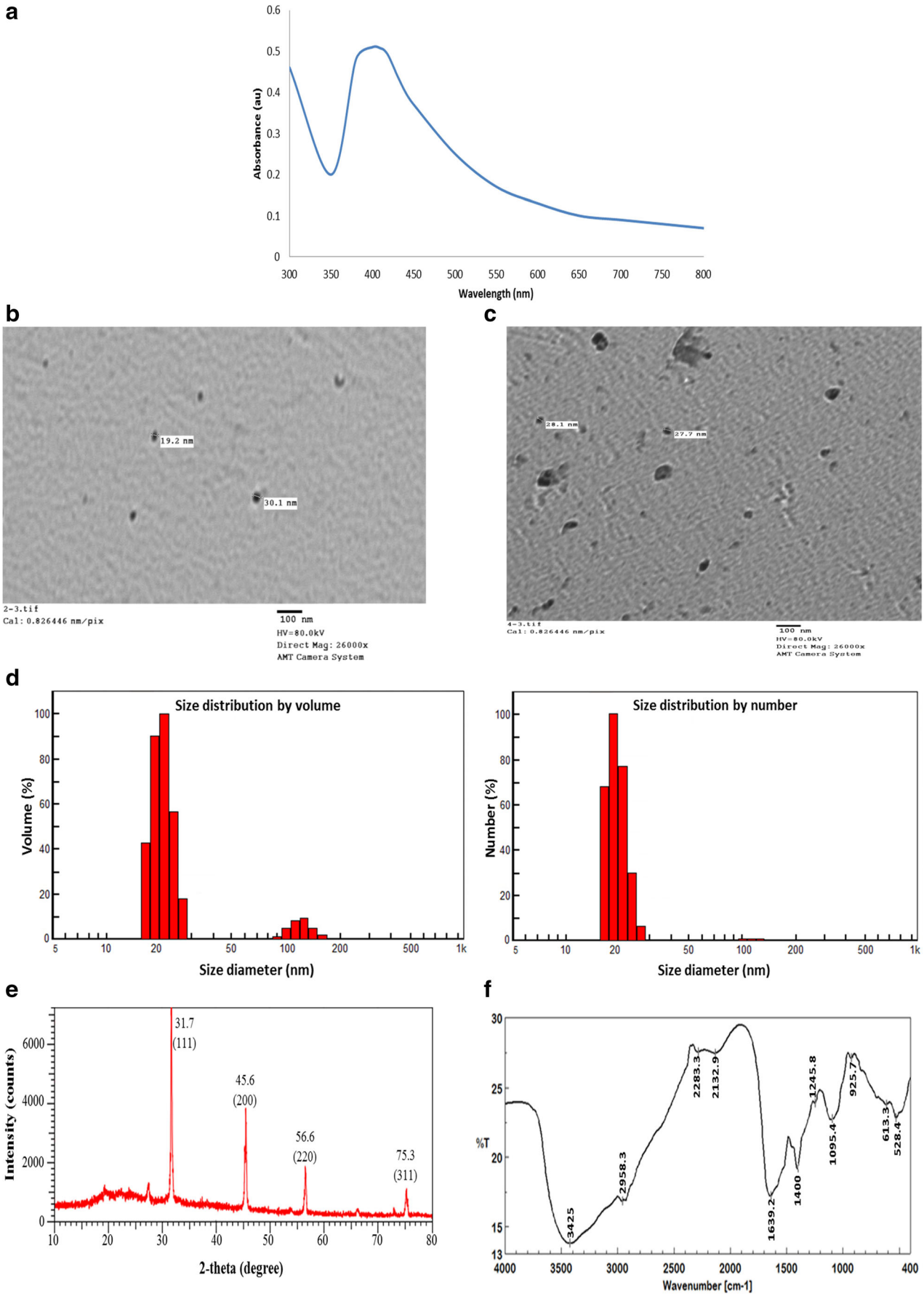
a
Absorbance (au)
Wavelength (nm)
b
19.2 nm
30.1 nm
2-3.tif
Cal: 0.826446 nm/pix
100 nm
HV=80.0kV
Direct Mag: 26000x
AMT Camera System
c
28.1 nm
27.7 nm
4-3.tif
Cal: 0.826446 nm/pix
100 nm
HV=80.0kV
Direct Mag: 26000x
AMT Camera System
d
Size distribution by volume
Volume (%)
Size diameter (nm)
Size distribution by number
Number (%)
Size diameter (nm)
e
Intensity (counts)
31.7
(111)
45.6
(200)
56.6
(220)
75.3
(311)
2-theta (degree)
f
%T
3425
2958.3
2283.3
2132.9
1639.2
1400
1245.8
1095.4
925.7
613.3
528.4
Wavenumber [cm-1]

◀ **Fig. 1** Characterization of AgNPs phytosynthesized by Burgu extract (pH 7, room temperature, 14 h). **a** UV-visible spectrum of AgNPs showing strong absorption peak at 405 nm. **b** TEM micrograph of AgNPs. **c** TEM micrograph of AgNPs after 30 days. **d** DLS analysis of AgNPs showing AgNPs size distribution by volume (left) and number (right). **e** XRD spectra of AgNPs. **f** FTIR spectra of AgNPs

antibacterial assays include increased sensitivity and ability to distinguish between bacteriostatic and bactericidal effects [46]. The inhibitory activity of AgNPs was examined visually by the color change of the resazurin indicator. The MBC is the minimum concentration of biosynthesized AgNPs which required to kill the bacterium completely under specific conditions (showed no growth on the agar plate) [47]. MBC for *P. aeruginosa* and *K. oxytoca* were observed at 25 and 50 μg/mL of AgNPs, respectively (Table 1). Antibacterial agents are usually regarded as bactericidal if the MBC/MIC ratio is ≤4 and bacteriostatic if >4 [30]. The MBC/MIC ratios of AgNPs were equal to 4 for both two tested isolates, indicating bactericidal activity. A previous study strongly supports our antibacterial data of AgNPs against MDR gram-negative bacteria [48]. The bactericidal effect of AgNPs is likely to become important therapeutic and clinical options very soon, especially with that growing multidrug resistance in bacteria. The antibacterial effect of AgNPs is attributed to their ultrafine sizes and larger surface area, which enable AgNPs to penetrate and destroy the cellular membranes, resulting in leaking of cellular contents. By penetrating into the cytoplasm, AgNPs convert to silver ions which damage the intracellular structures, impair cellular respiration functions, inactivate of cellular enzymes via interaction with thiol-containing proteins, and generate reactive oxygen species to induce oxidative stress and damaging of nucleic acids and proteins and eventually causing cell death [34, 40, 43].

3.2.2 Time-Kill Kinetics Assay

The time-kill kinetics profile of the biosynthesized AgNPs against *K. oxytoca* (ATCC 51983) and *P. aeruginosa* (ATCC MP-23) revealed gradual reduction in number of viable cells (CFU/mL) over the course of time. This reduction was dependent on time and AgNPs concentrations (Fig. 3). The number of CFU/mL for both *K. oxytoca* and *P. aeruginosa* was reduced by 2-log10 at (2×) MIC, 3-log10 at (4×) MIC, and 4-log10 at 8× MIC of AgNPs at 2 h. The bactericidal endpoint of AgNPs for *K. oxytoca* was reached after 8 and 12 h of incubation with (8×) MIC (50μg/mL) and (4×) MIC (25 μg/mL), respectively. While for *P. aeruginosa*, the bacteria were killed at (8×) MIC (100 μg/mL) of AgNPs at 6 h. At concentrations up to (4×) MIC, AgNPs did not have any bactericidal activity at 12 h against *P. aeruginosa*. Similar observations were observed for *K. oxytoca* but with lower AgNP concentrations up to (4×) MIC. However, although the endpoint reached faster after at (8×) MIC, no significant differences (P>0.05) were found among the two tested bacteria. Overall, results showed broad spectrum activity of green-synthesized AgNPs against the tested MDR bacteria. Green-synthesized AgNPs consider potent antibacterial agents due to their strong biocidal effect against different tested microorganism. Agnihotri et al. [49] stated that the antibacterial activity was improved when NPs were applied, and the fastest antibacterial effect was recorded with particle size less than 10 nm.

In this study, our green-synthesized AgNPs efficiently reduced the growth of bacteria (approximately 10^6 CFU/mL), indicating that AgNPs have a good antibacterial activity against MDR gram-negative bacteria. Both of tested MDR gram-negative bacteria were affected within short time and low concentrations; this may be due to the thinner cell wall composition compared to gram-positive bacteria. Green-synthesized AgNPs are more advantageous when compared to traditional chemicals with antimicrobial properties. Traditional chemicals involved in antimicrobial drugs are limited by specific binding of the microorganisms with the surface and metabolites of the antimicrobial agents. The increased usage of antibiotics led to the development of generations of antibiotic-resistant microorganisms within a short period of time. So, green-synthesized AgNPs could be an effective and alternative therapy to overcome the widespread of MDR microorganisms.

Table 1 Diameters of zones of inhibition (mm), minimum inhibitory concentration (MIC), and minimum bactericidal concentration (MBC) of AgNPs phytosynthesized by Burgu extract against human pathogenic multidrug-resistant *Klebsiella oxytoca* ATCC 51983 and *Pseudomonas aeruginosa* ATCC MP-23. The experiments were done in triplicates and data were presented as ±SD

Bacteria	Zones of inhibition (mm)					MIC (μg/mL)	MBC (μg/mL)	MBC/MIC ratio	Effect
	AgNPs (μg/mL)		CIP	Plant extract	$AgNO_3$				
	25	50							
K. oxytoca ATCC 51983	14	15	ND	ND	ND	6.25	25	4	Bactericidal
P. aeruginosa ATCC MP-23	15	19	ND	ND	ND	12.5	50	4	Bactericidal

CIP, ciprofloxacin; *ND*, not detected

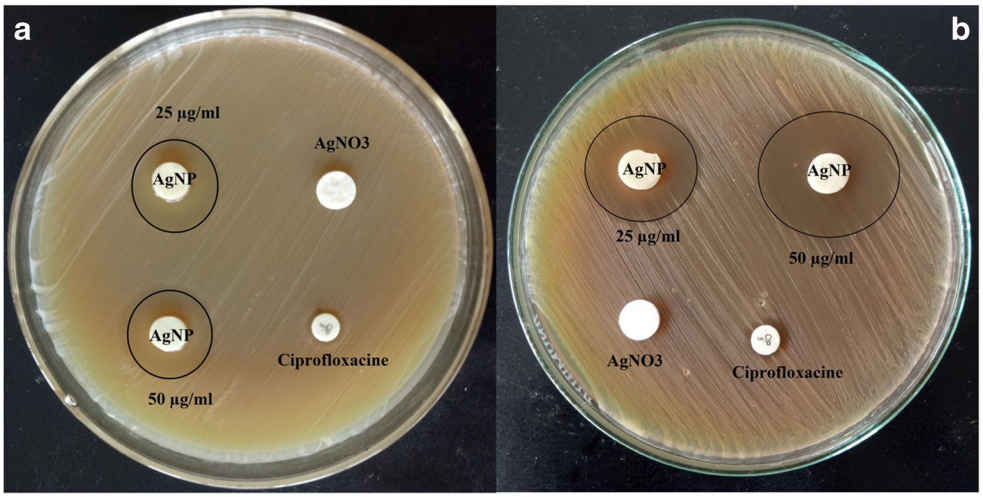

Fig. 2 In vitro anti-bacterial activity of AgNPs phytosynthesized by Burgu extract against human pathogenic multidrug-resistant strains: *Klebsiella oxytoca* ATCC 51983 (**a**) and *Pseudomonas aeruginosa* ATCC MP-23 (**b**). AgNPs were used at concentrations of 25 and 50 µg/mL. $AgNO_3$ solution and ciprofloxacin (CIP) were used as controls. The measurements were done in triplicates for each sample

3.3 In Vitro Cytotoxicity Assessment of AgNPs

It is well understood and firmly established that liver cells are the predominant cells for trapping and accumulation of AgNPs, causing serious hepatotoxicity. Therefore, hepatoma cell line HepG2 was used to investigate the cytotoxicity of green-synthesized AgNPs. In this study, we employed dose-dependent approach of biosynthesized AgNPs (5, 10, 20, 40, 80, 160, 320, and 640 µg/mL) to carefully evaluate their in vitro potential cytotoxicity against HepG2 and normal Vero cell line. The cell viabilities (%) of AgNP-treated Vero cells were 99.5±1.1, 89.3±1.7, 76.2±2.4, 61.1±1.7, 54.4±1.8, 49±1.8, 33.1

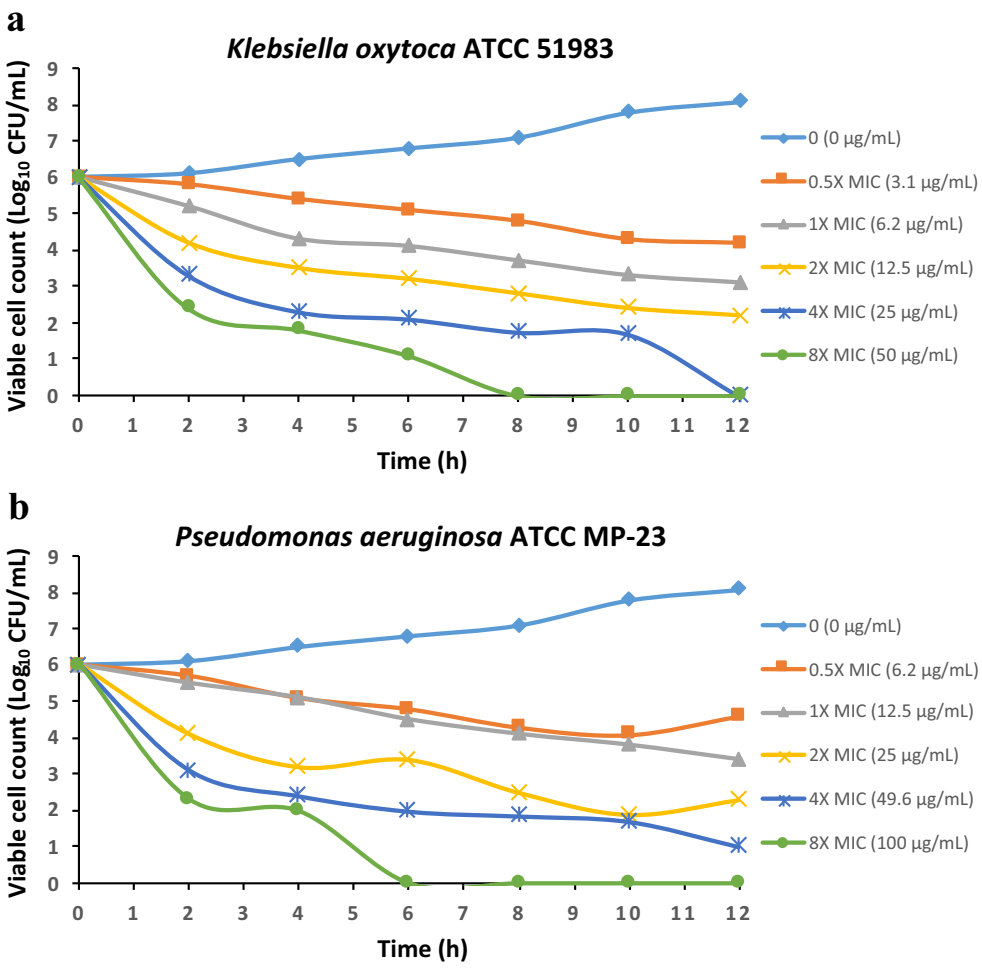

Fig. 3 Time-kill plots of AgNPs phytosynthesized by Burgu extract against human pathogenic multidrug-resistant strains: *Klebsiella oxytoca* ATCC 51983 (**a**) and *Pseudomonas aeruginosa* ATCC MP-23 (**b**) at different concentrations and time-length. The experiment was performed in triplicate and a graph of the log CFU/mL was plotted against time

±1.1, and 28.5±0.9% corresponding to AgNP concentrations of 5, 10, 20, 40, 80, 160, 320, and 640 μg/mL, respectively. Cytotoxicity effect of AgNPs against Vero cell line exhibited lowest toxicity with IC_{50} of 89.01 μg mL^{-1}, which indicate that no cytotoxic efficacy was observed on Vero cell line (Fig. 4a). The cell viabilities (%) of AgNP-treated HepG2 were 97.3±2.1, 92.6±1.7, 84.8±3.4, 45.2±3.7, 23.5±1.3, 18±1.4, 12.8±2.1, and 9.28±0.9% corresponding to AgNP concentrations of 5, 10, 20, 40, 80, 160, 320, and 640 μg/mL, respectively. Data showed that AgNPs significantly inhibited the viability of HepG2 cells in a dose-dependent manner (Fig. 4a). The IC_{50} value or the lowest concentration of AgNPs that inhibits 50% of HepG2 cells was at 35.1 μg/mL; the maximum cell death was found at the concentration of 640 μg/mL after 24 h of exposure to AgNPs. Similarly, Singh and colleagues demonstrated a dose-dependent cytotoxicity with an IC_{50} value of 20 μg/mL to HepG2 cells treated for 24 h with spherical AgNPs (10–50nm in size) bio-fabricated by Morus alba leaf extract [32]. Jacob et al. revealed cytotoxic effect with IC_{50} of 31.25 μg/mL against HepG2 cells for green spherical AgNPs (size 17.6–41 nm) biosynthesized using the extract of *Piper longum* leaf as reducing as well as capping agent [35]. Ahmadian et al. prepared AgNPs using chemical reduction

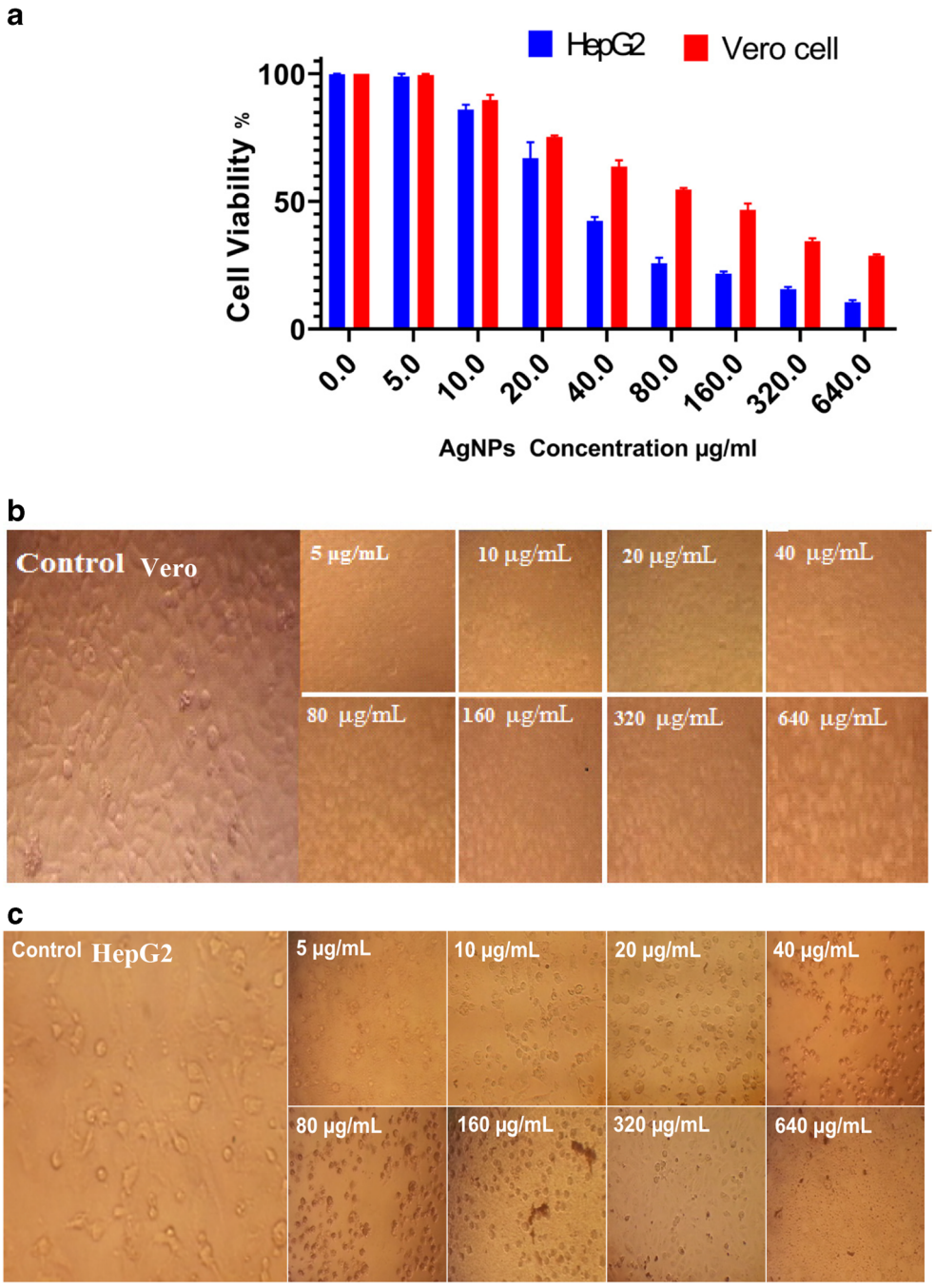

Fig. 4 In vitro anti-proliferative effect of AgNPs phytosynthesized by Burgu extract against Vero and HepG2 cells at twofold concentrations of AgNPs (5, 10, 20, 40, 80, 160, 320, and 640 μg/mL) for 24 h. **a** Viability percent for HepG2 cells treated by AgNPs as confirmed by MTT assay. Morphological changes of AgNPs-treated Vero (**b**) and HepG2 (**c**) cell lines (×10 magnification). The experiments were repeated three times and data were presented ±SD

methods [50]. They demonstrated toxicity of spherical AgNPs (30.7 nm) against HepG2 cells with IC_{50} value of 75 μg/mL. Our green AgNPs showed more toxic at lower concentrations than chemically produced AgNPs. Data revealed dose response reduction in the viability of HepG2 cell as visualized by inverted microscopy as shown in Fig. 4c. Microscopic observations exhibited dose-dependent morphological changes in AgNP-treated HepG2 cells compared to untreated ones. These morphological abnormalities were substantially varied from partial or complete losing of cytoskeleton monolayer shape, mounting of floating cells, malformation of cells epithelial-like shape to shrinkage, and cell granulation. It was suggested that the cytotoxicity effect of AgNPs is basically due to their nano-sized, by which AgNPs penetrate to the cytoplasm, nuclei, and other organelles, causing damage to the internal organelles and proteins of the cells and initiation of different immunological reactions. Moreover, AgNPs encourage formation of intercellular reactive oxygen species, and diminish cell proliferation and eventually apoptosis [35, 39, 43].

3.4 Mosquito Larvicidal Assay

Mosquitoes are the main vectors of many pathogens that cause severe mosquito-borne diseases and millions of deaths worldwide. *Anopheles pharoensis* and *Culex pipiens* mainly transmit several endemic diseases like lymphatic filariasis, malaria, yellow fever, and dengue fever to humans [49]. Recently, green-synthesized nanoparticles using plant extracts and their bioactive compounds showed promising mosquito larvicidal activities [50, 51]. For this study, it was of interest to investigate whether the green-synthesized AgNPs hold larvicidal activity or not. To this end, larvae of *A. pharoensis* and *C. pipiens* were treated with increasing concentrations of AgNPs (50–600 mg/mL). Data revealed that almost all AgNP-treated larvae of *A. pharoensis* and *C. pipiens* were dead 72 h post-treatment. The recorded LC_{50} and LC_{90} values were (87.669 and 538.017 mg/mL, respectively) for *A. pharoensis* and (51.338 and 311.227 mg/mL, respectively) for *C. pipiens* as shown in Table 2.

The mosquito larvicidal potency of Burgu extract green-synthesized AgNPs (LC_{50} ranging from 51.338 to 87.669 ppm) in our study is greater than or similar to that of extracts from related plants, since studies on the same plant are almost unavailable. Arial parts from five Lamiaceae plant extracts possess larvicidal activity against *Culex quinquefasciatus* with LC_{50} value ranged from 18.6 to 81.0 ppm [52]. The silver nanoparticles synthesized from *Belosynapsis kewensis* leaf extract were highly toxic against *A. stephensi* and *Ae. aegypti* larvae with LC_{50} of 78.4 and 84.2 ppm, respectively [53]. The mosquito larvicidal potential of green-synthesized silver nanoparticles by using *Annona glabra* leaves demonstrated significant larvicidal activity against *Aedes aegypti* and *Ae. albopictus* with LC_{50} values ranged from 2.43 to 5.94 mg/L [54]. In addition, our findings are in line with Rajakumar and Rahuman [55], who examined the effects of green-synthesized AgNPs towards 3rd larval instar of *C. quinquefasciatus* and *Anopheles subpictus*, elucidated suggestive larvicidal potentiality of green synthesized AgNPs with comparable LC_{50} values.

The AgNPs itself was found to be nontoxic to mosquito larvae as no mortality was seen in the group treated with AgNPs without plant extract. The low larvicidal concentrations of green-synthesized AgNPs may be attributed to their nano-sized particles which allow them easily penetration through cellular membrane, mitochondria, or even DNA that eventually lead to denaturation of proteins and nucleic acids [56]. A supportive evidence for this was provided by Rajkumar et al. [57] showing that nanoparticles enter mosquito tissues through the mitochondria and nucleus, revealing high toxicity of green-synthesized AgNPs against treated mosquitoes even with small concentrations. However, the larvicidal activity of tested extracts might be due to several phytochemicals these extracts may possess. The most active compound from Burgu extracts has not been elucidated yet and it

Table 2 Mosquito larvicidal activity of the crude and phytosynthesized Burgu extract AgNPs against *Anopheles pharoensis* and *Culex pipiens* mosquitoes

Insect	Treatment	LC_{50} (LCL–UCL) (mg/L)	LC_{90} (LCL–UCL) (mg/L)	χ^2	*df*
Anopheles pharoensis	Control	Nil	Nil	Nil	Nil
	AgNPs	Nil	Nil	Nil	Nil
	Crude extract	516.031 (390.844–1001.731)	3022.832 (2139.304–4983.771)	9.071 n.s.	3
	AgNPs	87.699 (53.206–170.514)	538.017 (416.688–1871.033)	3.201 n.s.	3
Culex pipiens	Control	Nil	Nil	Nil	Nil
	AgNPs	Nil	Nil	Nil	Nil
	Crude extract	373.235 (267.992–583.023)	1839.114 (1655.108–5830.221)	5.023 n.s.	3
	AgNPs	51.338 (31.728–109.114)	311.227 (260.110–474.553)	2.106 n.s.	3

LC_{50} concentration kills 50% of treated population, *LC_{90}* concentration kills 90% of treated population, *LCL* 95% lower confidence limits, *UCL* 95% upper confidence limits, χ^2 Chi square, *n.s.* not significant at $P>0.05$ level, *df* degrees of freedom, *Nil* nil mortality

may become a novel mosquito control agent that help in mosquito control programs. Overall, the obtained low lethal concentrations in this study open the way for further investigations and development of such environmentally safe insecticide instead of chemical insecticides.

4 Conclusion

In conclusion, an eco-friendly and cost-effectively phytosynthesis of AgNPs was carried out using *Echinochloa stagnina* (Retz.) P. Beauv. (Burgu) extract. Biosynthesized AgNPs were characterized by UV-Vis, TEM, DLS, XRD, and FTIR. Green-synthesized AgNPs were stable, monodisperse, nanocrystalline in nature, and with average size of 30 nm. FTIR signature showed that biomolecules in Burgu extract could be participated in the bio-reduction of Ag ions to AgNPs and in stabilization of AgNPs too. The phytosynthesized AgNPs revealed antibacterial activities against the two tested MDR bacteria (*Klebsiella oxytoca* ATCC 51983 and *Pseudomonas aeruginosa* ATCC MP-23), antitumor activity against HepG2 and larvicidal activity against *Anopheles pharoensis* and *Culex pipiens* mosquitoes.

Funding None.

Declarations

Conflict of Interest The authors declare no competing interests.

Research Involving Humans and Animals Statement None.

Informed Consent None.

References

1. Elegbede, J. A., & Lateef, A. (2019). Green synthesis of silver (Ag), gold (Au) and silver-gold (Ag-Au) alloy nanoparticles: a review on recent advances, trends, and biomedical applications. *Nanotechnology and Nanomaterial Applications in Food, Health, and Biomedical Sciences, 23*, 3–89. https://doi.org/10.1201/9780429425660-1.
2. Lateef, A., Elegbede, J. A., Akinola, P. O., & Ajayi, V. A. (2019). Biomedical applications of green synthesized-metallic nanoparticles: a review. *Pan Afr. J. Life Sci, 3*, 157–182. https://doi.org/10.36108/pajols/9102/30(0170).
3. Lateef, A., Ojo, S. A., Elegbede, J. A., Akinola, P. O., & Akanni, E. O. (2018). Nanomedical applications of nanoparticles for blood coagulation disorders. *Environmental Nanotechnology, pp.*, 243–277. https://doi.org/10.1007/978-3-319-76090-2_8.
4. Zhang, S., Tang, Y., & Vlahovic, B. (2016). A review on preparation and applications of silver-containing nanofibers. *Nanoscale Research Letters, 11*(1), 80. https://doi.org/10.1186/s11671-016-1286-z.
5. Jamkhande, P. G., Ghule, N. W., Bamer, A. H., & Kalaskar, M. G. (2019). Metal nanoparticles synthesis: an overview on methods of preparation, advantages and disadvantages, and applications. *Journal of Drug Delivery Science and Technology, 53*, 101174. https://doi.org/10.1016/j.jddst.2019.101174.
6. Shah, M., Fawcett, D., Sharma, S., Tripathy, S. K., & Poinern, G. E. J. (2015). Green synthesis of metallic nanoparticles via biological entities. *Materials, 8*(11), 7278–7308. https://doi.org/10.3390/ma8115377.
7. Rajeshkumar, S., & Bharath, L. V. (2017). Mechanism of plant-mediated synthesis of silver nanoparticles–a review on biomolecules involved, characterisation and antibacterial activity. *Chemico-Biological Interactions, 273*, 219–227. https://doi.org/10.1016/j.cbi.2017.06.019.
8. Fahimirad, S., Ajalloueian, F., & Ghorbanpour, M. (2019). Synthesis and therapeutic potential of silver nanomaterials derived from plant extracts. *Ecotoxicology and Environmental Safety, 168*, 260–278. https://doi.org/10.1016/j.ecoenv.2018.10.017.
9. Chand, K., Cao, D., Fouad, D. E., Shah, A. H., Dayo, A. Q., Zhu, K., Lakhan, M. N., Mehdi, G., & Dong, S. (2020). Green synthesis, characterization and photocatalytic application of silver nanoparticles synthesized by various plant extracts. *Arabian Journal of Chemistry*. https://doi.org/10.1016/j.arabjc.2020.01.009.
10. Brusotti, G., Cesari, I., Dentamaro, A., Caccialanza, G., & Massolini, G. (2014). Isolation and characterization of bioactive compounds from plant resources: the role of analysis in the ethnopharmacological approach. *Journal of Pharmaceutical and Biomedical Analysis, 87*, 218–228. https://doi.org/10.1016/j.jpba.2013.03.007.
11. Choudhury, R., Majumder, M., Roy, D. N., Basumallick, S., & Misra, T. K. (2016). Phytotoxicity of Ag nanoparticles prepared by biogenic and chemical methods. *International Nano Letters, 6*(3), 153–159. https://doi.org/10.1007/s40089-016-0181-z.
12. Adelere, I. A., & Lateef, A. (2016). A novel approach to the green synthesis of metallic nanoparticles: the use of agro-wastes, enzymes, and pigments. *Nanotechnology Reviews, 5*(6), 567–587. https://doi.org/10.1515/ntrev-2016-0024.
13. Ado, M. N., Guero, Y., Michot, D., Soubeiga, B., Kiesse, T. S., & Walter, C. (2016). Phytodesalinization of irrigated saline Vertisols in the Niger Valley by Echinochloa stagnina. *Agricultural Water Management, 177*, 229–240. https://doi.org/10.1016/j.agwat.2016.07.024.
14. Brink, M. (2006). *Echinochloa stagnina* (Retz.) P. Beauv. In M. Brink & G. Belay (Eds.), *PROTA (Plant Resources of Tropical Africa / Ressources végétales de l'Afrique tropicale)*. Netherlands: Wageningen.
15. Abo-State, M. A., Mahdy, H. M., Ezzat, S. M., Abd El Shakour, E. H., & El-Bahnasawy, M. A. (2012). Antimicrobial resistance profiles of Enterobacteriaceae isolated from Rosetta Branch of river Nile, Egypt. *World Applied Sciences Journal, 19*(9), 1234–1243. https://doi.org/10.5829/idosi.wasj.2012.19.09.2785.
16. Ezzat, S. M., Abo-State, M. A., Mahdy, H. M., & Abd EL-Shakour, E.H. and El-Bahnasawy, M.A. (2014). The effect of ionizing radiation on multi-drug resistant *Pseudomonas aeruginosa* isolated from aquatic environments in Egypt. *British Microbiology Research Journal, 4*(8), 856–868. https://doi.org/10.9734/BMRJ/2014/7606.
17. Boateng, J., & Catanzano, O. (2020). Silver and silver nanoparticle-based antimicrobial dressings. *Therapeutic Dressings and Wound Healing Applications*, pp.157-184. https://doi.org/10.1002/9781119433316.ch8.
18. Bernhard, L., Bernhard, P., & Magnussen, P. (2003). Management of patients with lymphoedema caused by filariasis in North-eastern Tanzania: alternative approaches. *Physiotherapy, 89*(12), 743–749. https://doi.org/10.1016/S0031-9406(05)60500-7.

19. Benelli, G., & Beier, J. C. (2017). Current vector control challenges in the fight against malaria. *Acta Tropica, 174*, 91–96. https://doi.org/10.1016/j.actatropica.2017.06.028.
20. Lateef, A., Ojo, S. A., Akinwale, A. S., Azeez, L., Gueguim-Kana, E. B., & Beukes, L. S. (2015). Biogenic synthesis of silver nanoparticles using cell-free extract of Bacillus safensis LAU 13: antimicrobial, free radical scavenging and larvicidal activities. *Biologia, 70*(10), 1295–1306. https://doi.org/10.1515/biolog-2015-0164.
21. Lateef, A., Azeez, M. A., Asafa, T. B., Yekeen, T. A., Akinboro, A., Oladipo, I. C., Azeez, L., Ojo, S. A., Gueguim-Kana, E. B., & Beukes, L. S. (2016). Cocoa pod extract-mediated biosynthesis of silver nanoparticles: its antimicrobial, antioxidant and larvicidal activities. *Journal of Nanostructure in Chemistry, 6*(2), 159–169. https://doi.org/10.1007/s40097-016-0191-4.
22. Azeez, M. A., Lateef, A., Asafa, T. B., Yekeen, T. A., Akinboro, A., Oladipo, I. C., Gueguim-Kana, E. B., & Beukes, L. S. (2017). Biomedical applications of cocoa bean extract-mediated silver nanoparticles as antimicrobial, larvicidal and anticoagulant agents. *Journal of Cluster Science, 28*(1), 149–164. https://doi.org/10.1007/s10876-016-1055-2.
23. Aina, D. A., Owolo, O., Lateef, A., Aina, F. O., Hakeem, A. S., Adeoye-Isijola, M., Okon, V., Asafa, T. B., Elegbede, J. A., Olukanni, O. D., & Adediji, I. (2019). Biomedical applications of Chasmanthera dependens stem extract mediated silver nanoparticles as antimicrobial, antioxidant, anticoagulant, thrombolytic, and larvicidal agents. *Karbala International Journal of Modern Science, 5*(2), 71–80. https://doi.org/10.33640/2405-609X.1018.
24. Thiyagarajan, P., Kumar, P., Kovendan, K., & Murugan, K. (2014). Effect of medicinal plant and microbial insecticides for the sustainable mosquito vector control. *Acta Biologica Indica., 3*(1), 527–535.
25. Benelli, G., Caselli, A., & Canale, A. (2017). Nanoparticles for mosquito control: challenges and constraints. *Journal of King Saud University-Science., 29*(4), 424–435. https://doi.org/10.1016/j.jksus.2016.08.006.
26. Govindarajan, M., Rajeswary, M., Muthukumaran, U., Hoti, S. L., Khater, H. F., & Benelli, G. (2016). Single-step biosynthesis and characterization of silver nanoparticles using Zornia diphylla leaves: a potent eco-friendly tool against malaria and arbovirus vectors. *Journal of Photochemistry and Photobiology B: Biology, 161*, 482–489. https://doi.org/10.1016/j.jphotobiol.2016.06.016.
27. Theerthavathy, B.S., Arakhanum, S., Kumar, B.R. and Kiran, S.R., 2019. Anti-oxidant and anti-microbial activities of silver nanoparticles of essential oil extracts from leaves of Zanthoxylum ovalifolium. *European Journal of Medicinal Plants*, pp.1-11. https://doi.org/10.9734/ejmp/2019/v29i330157
28. Travnickova, E., Mikula, P., Oprsal, J., Bohacova, M., Kubac, L., Kimmer, D., Soukupova, J., & Bittner, M. (2019). Resazurin assay for assessment of antimicrobial properties of electrospun nanofiber filtration membranes. *AMB Express, 9*(1), 183. https://doi.org/10.1186/s13568-019-0909-z.
29. Shehabeldine, A., & Hasanin, M. (2019). Green synthesis of hydrolyzed starch–chitosan nano-composite as drug delivery system to gram negative bacteria. *Environmental Nanotechnology, Monitoring & Management, 12*, 100252. https://doi.org/10.1016/j.enmm.2019.100252.
30. Keepers, T. R., Gomez, M., Celeri, C., Nichols, W. W., & Krause, K. M. (2014). Bactericidal activity, absence of serum effect, and time-kill kinetics of ceftazidime-avibactam against β-lactamase-producing Enterobacteriaceae and Pseudomonas aeruginosa. *Antimicrobial Agents and Chemotherapy, 58*(9), 5297–5305. https://doi.org/10.1128/AAC.02894-14.
31. Farag, M. M., Moghannem, S. A., Shehabeldine, A. M., & Azab, M. S. (2020). Antitumor effect of exopolysaccharide produced by Bacillus mycoides. *Microbial Pathogenesis, 140*, 103947. https://doi.org/10.1016/j.micpath.2019.103947.
32. Medda, S., Hajra, A., Dey, U., Bose, P., & Mondal, N. K. (2015). Biosynthesis of silver nanoparticles from Aloe vera leaf extract and antifungal activity against Rhizopus sp. and Aspergillus sp. *Applied Nanoscience, 5*(7), 875–880. https://doi.org/10.1007/s13204-014-0387-1.
33. Singh, A., Dar, M. Y., Joshi, B., Sharma, B., Shrivastava, S., & Shukla, S. (2018). Phytofabrication of silver nanoparticles: novel drug to overcome hepatocellular ailments. *Toxicology Reports, 5*, 333–342. https://doi.org/10.1016/j.toxrep.2018.02.013.
34. Chouhan, S., & Guleria, S. (2020). Green synthesis of AgNPs using Cannabis sativa leaf extract: characterization, antibacterial, antiyeast and α-amylase inhibitory activity. *Materials Science for Energy Technologies*. https://doi.org/10.1016/j.mset.2020.05.004.
35. Jacob, S. J. P., Finub, J. S., & Narayanan, A. (2012). Synthesis of silver nanoparticles using Piper longum leaf extracts and its cytotoxic activity against Hep-2 cell line. *Colloids and Surfaces B: Biointerfaces, 91*, 212–214. https://doi.org/10.1016/j.colsurfb.2011.11.001.
36. Dakshayani, S. S., Marulasiddeshwara, M. B., Kumar, S., Golla, R., Devaraja, S. R. H. K., & Hosamani, R. (2019). Antimicrobial, anticoagulant and antiplatelet activities of green synthesized silver nanoparticles using Selaginella (Sanjeevini) plant extract. *International Journal of Biological Macromolecules, 131*, 787–797. https://doi.org/10.1016/j.ijbiomac.2019.01.222.
37. Pirtarighat, S., Ghannadnia, M., & Baghshahi, S. (2019). Green synthesis of silver nanoparticles using the plant extract of Salvia spinosa grown in vitro and their antibacterial activity assessment. *Journal of Nanostructure in Chemistry, 9*(1), 1–9. https://doi.org/10.1007/s40097-018-0291-4.
38. Ahmad, A., Syed, F., Shah, A., Khan, Z., Tahir, K., Khan, A. U., & Yuan, Q. (2015). Silver and gold nanoparticles from Sargentodoxa cuneata: synthesis, characterization and antileishmanial activity. *RSC Advances, 5*(90), 73793–73806. https://doi.org/10.1039/C5RA13206A.
39. Prasannaraj, G., Sahi, S. V., Ravikumar, S., & Venkatachalam, P. (2016). Enhanced cytotoxicity of biomolecules loaded metallic silver nanoparticles against human liver (HepG2) and prostate (PC3) cancer cell lines. *Journal of Nanoscience and Nanotechnology, 16*(5), 4948–4959. https://doi.org/10.1166/jnn.2016.12336.
40. Elmusa, F., Aygun, A., Gulbagca, F., Seyrankaya, A., Göl, F., Yenikaya, C., & Sen, F. (2020). Investigation of the antibacterial properties of silver nanoparticles synthesized using Abelmoschus esculentus extract and their ceramic applications. *International Journal of Environmental Science and Technology*, pp.1-12. https://doi.org/10.1007/s13762-020-02883-x.
41. El-Seedi, H. R., El-Shabasy, R. M., Khalifa, S. A., Saeed, A., Shah, A., Shah, R., Iftikhar, F. J., Abdel-Daim, M. M., Omri, A., Hajrahand, N. H., & Sabir, J. S. (2019). Metal nanoparticles fabricated by green chemistry using natural extracts: biosynthesis, mechanisms, and applications. *RSC Advances, 9*(42), 24539–24559. https://doi.org/10.1039/C9RA02225B.
42. Elbahnasawy, M. A., Shehabeldine, A. M., Khattab, A. M., Amin, B. H., & Hashem, A. H. (2021). *Green biosynthesis of silver nanoparticles using novel endophytic Rothia endophytica: characterization and anticandidal activity* (p. 102401). *Journal of Drug Delivery Science and Technology*. https://doi.org/10.1016/j.jddst.2021.102401.
43. Anjugam, M., Vaseeharan, B., Iswarya, A., Divya, M., Prabhu, N. M., & Sankaranarayanan, K. (2018). Biological synthesis of silver nanoparticles using β-1, 3 glucan binding protein and their antibacterial, antibiofilm and cytotoxic potential. *Microbial Pathogenesis, 115*, 31–40. https://doi.org/10.1016/j.micpath.2017.12.003.
44. Rajivgandhi, G. N., Ramachandran, G., Maruthupandy, M., Manoharan, N., Alharbi, N. S., Kadaikunnan, S., Khaled, J. M.,

Almana, T. N., & Li, W. J. (2020). Anti-oxidant, anti-bacterial and anti-biofilm activity of biosynthesized silver nanoparticles using Gracilaria corticata against biofilm producing K. pneumoniae. *Colloids and Surfaces A: Physicochemical and Engineering Aspects*, p.124830. https://doi.org/10.1016/j.colsurfa.2020.124830.

45. Shehabeldine, A. M., Ashour, R. M., Okba, M. M., & Saber, F. R. (2020). Callistemon citrinus bioactive metabolites as new inhibitors of methicillin-resistant Staphylococcus aureus biofilm formation. *Journal of Ethnopharmacology, 254*, 112669. https://doi.org/10.1016/j.jep.2020.112669.
46. Caleffi-Ferracioli, K. R., Maltempe, F. G., Siqueira, V. L. D., & Cardoso, R. F. (2013). Fast detection of drug interaction in Mycobacterium tuberculosis by a checkerboard resazurin method. *Tuberculosis, 93*(6), 660–663. https://doi.org/10.1016/j.tube.2013.09.001.
47. Das, P., Bose, M., Ganguly, S., Mondal, S., Das, A. K., Banerjee, S., & Das, N. C. (2017). Green approach to photoluminescent carbon dots for imaging of gram-negative bacteria Escherichia coli. *Nanotechnology*, *28*(19), p.195501. https://doi.org/10.1088/1361-6528/aa6714.
48. Cavassin, E. D., de Figueiredo, L. F. P., Otoch, J. P., Seckler, M. M., de Oliveira, R. A., Franco, F. F., Marangoni, V. S., Zucolotto, V., Levin, A. S. S., & Costa, S. F. (2015). Comparison of methods to detect the in vitro activity of silver nanoparticles (AgNP) against multidrug resistant bacteria. *Journal of nanobiotechnology*, *13*(1), p.64. https://doi.org/10.1186/s12951-015-0120-6.
49. WHO 2019: Mosquito-borne diseases. Available from: https://www.who.int/neglected_diseases/vector_ecology/mosquito-borne-diseases/en/
50. Sutthanont, N., Attrapadung, S., & Nuchprayoon, S. (2019). Larvicidal activity of synthesized silver nanoparticles from Curcuma zedoaria essential oil against Culex quinquefasciatus. *Insects*, *10*(1), p.27. https://doi.org/10.3390/insects10010027.
51. Saini, H., Yadav, R., Kumar, D., Kumar, G., & Agrawal, V. (2020). Cullen corylifolium (L.) Medik. Seed extract, an excellent system for fabrication of silver nanoparticles and their multipotency validation against different mosquito vectors and human cervical cancer cell line. *Journal of Cluster Science, 31*(1), 161–175. https://doi.org/10.1007/s10876-019-01630-8.
52. Cetin, H., Cinbilgel, I., Yanikoglu, A., & Gokceoglu, M. (2006). Larvicidal activity of some Labiatae (Lamiaceae) plant extracts from Turkey. *Phytotherapy Research: An International Journal Devoted to Pharmacological and Toxicological Evaluation of Natural Product Derivatives., 20*(12), 1088–1090. https://doi.org/10.1002/ptr.2004.
53. Bhuvaneswari, R., Xavier, R. J., & Arumugam, M. (2016). Larvicidal property of green synthesized silver nanoparticles against vector mosquitoes (*Anopheles stephensi* and *Aedes aegypti*). *Journal of King Saud University-Science., 28*(4), 318–323. https://doi.org/10.1016/j.jksus.2015.10.006.
54. Amarasinghe, L. D., Wickramarachchi, P. A. S. R., Aberathna, A. A. A. U., Sithara, W. S., & De Silva, C. R. (2020). Comparative study on larvicidal activity of green synthesized silver nanoparticles and *Annona glabra* (Annonaceae) aqueous extract to control *Aedes aegypti* and *Aedes albopictus* (Diptera: Culicidae). *Heliyon., 6*(6), e04322. https://doi.org/10.1016/2Fj.heliyon.2020.e04322.
55. Rajakumar, G., & Rahuman, A. A. (2011). Larvicidal activity of synthesized silver nanoparticles using Eclipta prostrata leaf extract against filariasis and malaria vectors. *Acta Tropica, 118*(3), 196–203. https://doi.org/10.1016/j.actatropica.2011.03.003.
56. Sareen, S.J., Pillai, R.K., Chandramohanakumar, N. and Balagopalan, M., 2012. Larvicidal potential of biologically synthesised silver nanoparticles against Aedes Albopictus. Res J Rec Sci, 1(ISC-2011), pp.52-56
57. Rajkumar, R., Shivakumar, M. S., Nathan, S. S., & Selvam, K. (2018). Pharmacological and larvicidal potential of green synthesized silver nanoparticles using Carmona retusa (Vahl) Masam leaf extract. *Journal of Cluster Science, 29*(6), 1243–1253. https://doi.org/10.1007/s10876-018-1443-x.